One-Pot Synthesis of Single-Crystal Palladium Nanoparticles with Controllable Sizes for Applications in Catalysis and Biomedicine

Yang Wang, †,‡ Alexander Biby,† Zheng Xi,† Bo Liu,‡ Qinchun Rao,§ Xiaohu Xia†,I,*

†Department of Chemistry, University of Central Florida, Orlando, Florida 32816, United States

[‡]Department of Chemistry, School of Science, Beijing Jiaotong University, Beijing 100044, P. R. China

§Department of Nutrition, Food and Exercise Sciences, Florida State University, Tallahassee, Florida 32306, United States

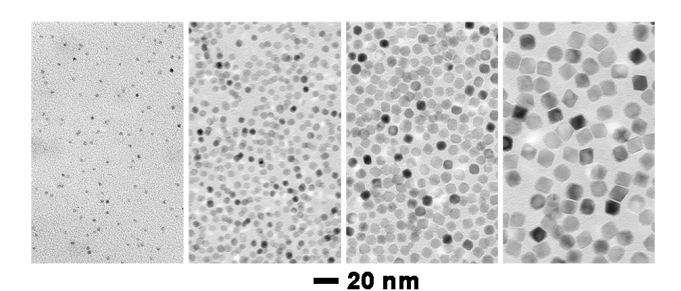
NanoScience Technology Center, University of Central Florida, Orlando, Florida 32816, United States

*Corresponding author. E-mail: Xiaohu.Xia@ucf.edu

Abstract

Palladium (Pd) nanoparticles are of particular interest to various fundamental studies and emerging areas of technology. The properties of Pd nanoparticles have a strong dependence on particle size. Nevertheless, it has been challenging to synthesize uniform Pd nanoparticles with controllable sizes and in relatively large quantities. Herein, we demonstrate a simple yet robust one-pot synthesis for the preparation of single-crystal Pd nanoparticles with controllable sizes in the range of 2 nm to 14 nm. The synthesis is simply performed by mixing polyvinylpyrrolidone (PVP), Na₂PdCl₄, and ethylene glycol in a glass vial that is placed in an oil bath with stirring. The sizes could be conveniently and tightly controlled by adjusting the amount of PVP or Na₂PdCl₄/PVP. The final products are highly uniform in terms of size and shape. Notably, the strategy of size control was successfully extended to Pt and Rh nanoparticles. The synthesis could be scaled up to allow for the production of gram-level quantities of Pd nanoparticles in a short period of time. The uniform Pd nanoparticles with controllable sizes are believed to find important use in different areas, such as fundamental nanoresearch, catalysis, and biomedicine.

Table of Contents



Keywords: palladium · nanoparticle · controlled synthesis · catalysis · overgrowth

INTRODUCTION

Palladium (Pd) nanoparticles have attracted enormous research interests in both academia and industry, owing to their fascinating physicochemical properties and broad applications in catalysis and recent biomedical studies.¹⁻⁶ It is well known that the physicochemical properties of Pd nanoparticles have a strong dependence on their size.⁷ For example, particle size was found to play vital roles in determining the catalytic performance of Pd nanoparticles in a number of important reactions, such as Suzuki cross-coupling reactions,^{8,9} hydrogenation reactions,^{10,11} CO oxidation,^{12,13} and oxidation of formic acid.^{14,15} Particle size also matters in biomedical applications of Pd nanoparticles. For instance, only if the size of Pd nanoparticles is ultra-small (< 10 nm) can they be cleared out from the body in high efficiencies via the renal excretion route.^{16,17} In another example, it was reported that the antimicrobial activities of Pd nanoparticles were highly size-dependent.¹⁸ A fine-scale differences in size (<1 nm) could alter their antimicrobial activities.

Driven by these and many other examples, it has become significant to develop synthetic protocols for producing Pd nanoparticles with a precise control over the size. Of particular interest is size control at the sub-ten nanometer regime, at which the impact of size on the physicochemical properties of Pd nanoparticles is more evident.^{19,20} Owing to the great work of many researchers, it is now experimentally feasible to generate Pd nanoparticles with different sizes.²¹⁻²⁵ Despite the successful demonstrations, we noticed that the synthesis of quality Pd nanoparticles having highly uniform shapes and narrow size distributions has been met with limited success. It should be mentioned that the uniformity of Pd nanoparticles could be improved by a two-step strategy known as seed-mediated growth, which allows for better control over the growth process of preformed seeds.²⁶⁻²⁸ Nevertheless, in comparison to one-pot synthesis, seed-mediated growth is less straightforward since it involves multiple steps.²⁹ In addition, seed-mediated growth is typically used to fabricate small quantities of nanoparticles, imposing the difficulties in producing nanoparticles at industrially relevant scales. Taken together, production of Pd nanoparticles with great uniformity and large quantity is important, yet challenging.

In this work, we report a facile one-pot synthesis of uniform Pd nanoparticles with controllable sizes in the range of approximately 2-14 nm. The synthetic system is simple which only involves three chemicals – polyvinylpyrrolidone (PVP), Na₂PdCl₄, and ethylene glycol

(EG). The synthesis was performed by simply adding 1.0 mL of Na₂PdCl₄ solution in EG to a glass vial containing 2.0 mL of PVP solution in EG that was preheated at 160 °C under magnetic stirring (see Figure 1 and Experimental Section for details). The size of Pd nanoparticles as final products could be conveniently controlled by varying the amount of PVP or Na₂PdCl₄/PVP in EG (Figure 1). The synthesis could be easily scaled up to produce quality Pd nanoparticles at gram-level quantities.

Our synthesis has several promising features that may make them widely applicable in the laboratory and industry: simple synthetic procedure (involvement of only three commonly used chemicals), production of nanoparticles with high purity (nearly 100%) and good uniformities (in terms of size, shape, and crystallinity), convenient control over nanoparticle size (by varying the amount of one or two chemicals), easy scale up (by simply increasing the amount of each chemical at the same scale), and applicability in size-controlled synthesis of Pt and Rh nanoparticles. In comparison, those previously reported one-pot syntheses of Pd nanoparticles oftentimes involved multiple chemicals/steps, production of non-uniform nanoparticles, and/or relatively complicated procedures for size control and scale up.^{21-25, 30-34}

EXPERIMENTAL SECTION

Chemicals and Materials. Sodium tetrachloroplatinate(II) hydrate (Na₂PtCl₄·xH₂O), sodium tetrachloropalladate(II) (Na₂PdCl₄, 98%), rhodium(III) chloride (RhCl₃), poly(vinylpyrrolidone) (PVP, $M_w \approx 55,000$), hydrochloric acid (HCl, 37%), and acetone (\geq 99.9%) were purchased from Sigma-Aldrich. Ethylene glycol (EG) was bought from J. T. Baker. The water used in all experiments was deionized (DI) water with a resistivity of 18.2 M Ω ·cm.

Synthesis of Pd Nanoparticles. In a standard synthesis of 5.3 nm Pd nanoparticles, 40 mg of PVP was dissolved in 2.0 mL of EG and was then put to a 20-mL glass vial. The vail was then put to a 160 °C oil bath for preheating under magnetic stirring. Then, 1.0 mL of Na₂PdCl₄ solution in EG (16 mg/mL) was quickly injected into the vial using a pipette. After 1 hour, the reaction was terminated by using an ice-water bath, to which the vial was immersed. The final products were washed one time with acetone and two times with DI water in order to remove excess reagents. For syntheses of Pd nanoparticles of other sizes, a similar procedure was used, except for the variations of the amounts of PVP and Na₂PdCl₄ as specified in Table 1.

Percent Conversions of Pd Precursor during the Synthesis. The amount of Na₂PdCl₄

remaining in the reaction solution was quantified using UV-vis spectroscopy.³⁵ Specifically, an aliquot of 0.1 mL was taken out of the reaction solution at t = 3 seconds by a pipette and quickly injected into 1.4 mL of 0.1 M HCl aqueous solution to quench the reaction and to prevent PdCl₄²⁻ from hydrolysis.³⁶ Then, Pd nanoparticles were separated from the solution through centrifugation. The supernatant was subject to UV-vis measurement after it had been diluted with 0.1 M HCl solution. The concentration of PdCl₄²⁻ left over in the reaction solution, which had an absorbance peak at 420 nm, could be derived by comparing to a calibration curve generated from PdCl₄²⁻ standards. Finally, percent conversion of Na₂PdCl₄ to Pd(0) was calculated from the concentrations of the remaining and initial PdCl₄²⁻.

Scale-up Synthesis. The 50-fold scale up synthesis was conducted in a 500 mL flask as the reaction container. A similar procedure as the standard synthesis was used, except that: *i*) the volumes of PVP and Na₂PdCl₄ solutions in EG were increased by 50 times, while their concentrations were kept the same as those in small scale synthesis; *ii*) the PVP solution was preheated in the oil bath for 30 min to ensure a thorough preheat; and *iii*) the Na₂PdCl₄ solution (50 mL) was poured to the reaction solution using a beaker.

Instrumentation. Transmission electron microscope (TEM) images were obtained from a JEOL JEM-1011 microscope operated at 100 kV. UV-vis absorption spectra were recorded using an Agilent Cary 60 UV-vis spectrophotometer. Concentrations of Pd element from Pd nanoparticles were measured using an inductively coupled plasma-mass spectrometry (ICP-MS, a JY2000 Ultrace ICP atomic emission spectrometer), in which Pd nanoparticles were dissolved and converted to Pd ions with aqua regia. X-ray diffraction (XRD) data was aquired from a Scintag XDS2000. An ultracentrifuge (Beckman Coulter Optima™ Max-XP Tabletop) was used for the centrifugation of all nanoparticles. The X-ray photoelectron spectroscopy (XPS) analyses were performed on a Physical Electronics 5400 system. Thermal gravimetric analysis (TGA) was performed with a Shimadzu's TGA-50 analyzer. In TGA analysis, sample at room temperature was heated to 600 °C (10°C per minute) and was kept at 600 °C for 30 minutes under nitrogen flow at 20 mL per minute.

RESULTS AND DISCUSSION

Synthesis of 5.3 nm Pd nanoparticles

We started with the standard synthesis (see Figure 1a and Experimental Section for details),

in which the amounts of Na₂PdCl₄ and PVP in EG were set to 16 and 40 mg, respectively. Figure 2a shows a typical low-magnification transmission electron microscopy (TEM) image of the final products prepared from a standard synthesis. The products were monodispersed nanoparticles with high purity and good uniformity. From Figure 2b (*i.e.*, a magnified TEM image), the shape of the products was resolved to be truncated octahedron. It is worth noting that truncated octahedron is a thermodynamically favored shape with minimal total surface free energy (*i.e.*, the so-called Wulff shape^{37,38}), implying the synthesis was under thermodynamic control.³⁹

Analyses on 200 random particles indicated that the average size (defined as the distance between two opposite {100} facets of a truncated octahedron, see Figure S1) of the final products was 5.3 nm. Figure 2c shows a high-resolution TEM (HRTEM) image of an individual Pd nanoparticle and the corresponding Fourier transform (FT) pattern, where periodic lattice fringes without twin boundaries could be clearly resolved. The lattice fringe spacing of 2.2 and 1.9 Å, respectively, could be assigned to the {111} and {200} crystal planes of face-centered cubic (fcc) Pd.⁴⁰ These observations suggested the final products were single-crystal Pd truncated octahedrons encased by both {100} and {111} facets.⁴¹ In the following discussion, the Pd truncated octahedrons as final products will be referred to as Pd nanoparticles for simplicity. XRD pattern of the same sample is shown in Figure 2d. All the peaks in the diffraction pattern could be indexed to fcc Pd (JCPDS no. 05-0681), confirming the nanoparticles were made of Pd and crystallized in an fcc structure. The quantity of Pd nanoparticles from one batch of synthesis was determined to be 5.68 mg by inductively coupled plasma-mass spectrometry (ICP-MS) analysis, indicating that 98.6% of the Pd precursor (i.e., Na₂PdCl₄) was converted to Pd nanoparticles.

To investigate surface properties of as-prepared Pd nanoparticles, we conducted X-ray photoelectron spectroscopy (XPS) analysis. Figure 2e shows the XPS survey spectra of the sample. The presence of peaks for C 1s, N 1s, O 1s, and Pd 3d suggested the chemisorption of PVP molecules on Pd surface. Figure 2f highlights the Pd 3d region of the XPS spectra, where weak Pd²⁺ peaks could be seen. The presence of Pd(II) species indicated that part of surface Pd atoms was oxidized. It should be mentioned that the absorbed PVP on Pd surface could effectively prevent nanoparticles from aggregation and ensure good water solubility for the nanoparticles, which is favored in many biomedical applications. In catalysis, however, PVP on

nanoparticle surface may hinder key reactive species from accessing to Pd surface. Previous studies demonstrated that the absorbed PVP could be effectively removed through UV-ozone treatment, thermal oxidation treatment, or chemical (*e.g.*, acid, base, and sodium borohydride) treatment. To quantitatively understand the absorbed PVP, we determined the packing density of PVP on the surface of as-prepared Pd nanoparticles through thermal gravimetric analysis (TGA). In TGA analysis, the sample was heated to 600 °C at a rate of 10 °C per minute. The loss of weight at range 350-550 °C could be ascribed to the combustion of PVP, while the weight leftover at 600 °C was from Pd. Based on the TGA data (Figure S2) and the size/shape of Pd nanoparticles (Figure 2b), the PVP packing density was roughly estimated to be 0.06 nm⁻² accordingly to the method described in our recent publication.

To gain insight into the formation of these Pd nanoparticles, aliquots of sample were taken out of a standard synthesis at different time, followed by the examination using TEM. In the early stage (t = 10 s, Figure S3a), the products were Pd nanoparticles with a relatively broad size distribution. Most of them were small particles of a few nanometers in size. The HRTEM image (see inset of Figure S3a) showed these small particles exhibited a quasi-circular profile and took a single crystal structure. At t = 30 s (Figure S3b), interestingly, the size distribution and uniformity of the nanoparticles had been greatly improved, implying the involvement of Ostwald ripening during the synthesis. 52,53 At this stage, the nanoparticles took an overall spherical shape with a diameter of ~3.9 nm. This observation suggests Ostwald ripening played a key role in ensuring the emergence of uniform products. When the reaction time was prolonged to 5 min, the average size of nanoparticles increased to ~4.9 nm (Figure S3c), while the shape remained the same. Thereafter (from 5 min to 1 h), the growth of nanoparticles became fairly slow. Eventually (t = 1 h, Figure S3d), the average size of nanoparticles reached ~ 5.3 nm. Notably, the nanoparticles had evolved to truncated octahedrons with distinguishable edges and corners. No obvious change in either the particle size or shape was observed when the reaction time was further extended.

Synthesis of 2-4 nm Pd nanoparticles

We then demonstrated that Pd nanoparticles with sizes smaller than 5.3 nm could be obtained by simply increasing the amount of PVP in a standard synthesis, while keeping all other reaction conditions unchanged (see Figure 1b and Table 1). For example, the size of Pd nanoparticles as final products reduced to 3.8 nm (Figure 3a) when the amount of PVP was increased from 40 to

200 mg. Importantly, the reduction of particle size did not compromise the uniformity of the nanoparticles. Further increase of PVP amount to 1,600 mg resulted in the formation of 2.1 nm Pd nanoparticles (Figure 3b) as final products. The inset of Figure 3b shows a typical HRTEM image of an individual nanoparticle. It can be seen that the nanoparticle was single-crystal Pd nanocrystal. It should be pointed out that, unlike the 5.3 nm Pd nanoparticles (Figure 2), the truncated octahedral shape could been barely resolved from these small-sized nanoparticles shown in Figure 3. Instead, they displayed an overall spherical shape. We assume the change of particle shape from truncated octahedron to sphere might be ascribed to the shrinkage of particle volume. It is known that volume shrinkage would increase the surface free energy of nanocrystals and thus promote the migration of atoms on edges/corners to the entire surface of a nanocrystal. Therefore, the final product tended to display a spherical shape. The additional low-magnification TEM images in Figures S4 demonstrate that both the 3.8 and 2.1 nm Pd nanoparticles could be obtained with high purities and good uniformities. Taken together, these results suggest that Pd nanoparticles with sizes smaller than 5.3 nm could be produced from the same synthetic system by simply increasing the amount of PVP.

Synthesis of 6-14 nm Pd nanoparticles

Based on the standard synthesis for 5.3 nm Pd nanoparticles, we demonstrated that Pd nanoparticles with larger sizes could be obtained by spontaneously increasing the amounts of Na₂PdCl₄ and PVP (see Figure 1c and Table 1). For instance, when 80 mg of Na₂PdCl₄ and 200 mg of PVP were used in the synthesis, the final products became 8.0 nm Pd nanoparticles (Figure 4a). As shown by Figure 4b-d and Table 1, the size of Pd nanoparticles as final products could be conveniently and precisely enlarged in the range of 8.0 – 14.4 nm by step-wisely increasing the amounts of Na₂PdCl₄ and PVP. It should be noted that further increase of Na₂PdCl₄ and PVP amounts led to the saturation of their EG solutions. The additional low-magnification TEM images (see Figure S5) of the samples shown in Figure 4 demonstrate that these Pd nanoparticles could be obtained with high purities and good uniformities. All these samples took nearly perfect Wulff shape. Compared to the 5.3 nm Pd nanoparticles shown in Figure 2, the edges and tips of these larger Pd nanoparticles are more evident.

Mechanistic understanding on size control

Generally, one-pot synthesis of metal nanocrystals involves the formation of seeds and subsequent growth as the two critical steps. 41,55 During a synthesis, salt precursors are reduced to

metal atoms. Once the concentration of metal atoms has reached the point of supersatuation, small clusters begin to appear through self-nucleation. These clusters will evolve into seeds through the autocatalytic effect, which will then serve as the active sites for subsequent crystal growth. The continuous growth of the seeds will eventually lead to the formation of metal nanocrystals as final products. Therefore, the size of the final product is primarily determined by the percentage of conversion from salt precursor to metal atoms at the initial stage of nucleation or seed formation. A greater percent conversion of precursor indicates the generation of a relatively larger number of seeds and thus the formation of smaller sized final products, and vice versa (see Figure 1).

To quantify such percent conversion of precursor at the initial stage of our synthetic system, we determined the concentrations of PdCl₄²⁻ ions by recording their UV-vis spectra.³⁵ Specifically, the reaction was quenched at t = 3 s using an ice-water bath when small clusters with sizes < 1 nm were formed (*i.e.*, the initial stage). Then the sample was centrifuged to remove precipitates. The supernatant was collected and diluted to a level suitable for UV-vis measurement. On the basis of the calibration curve generated from Na₂PdCl₄ solutions of known concentrations (see Figure S6), the percent conversion of Na₂PdCl₄ could be derived by comparing the amount of Na₂PdCl₄ remaining in reaction solution and the amount of initial Na₂PdCl₄ introduced to the reaction. Figure 5 summarizes the percent conversions of Na₂PdCl₄ at the initial stage for all Pd nanoparticles shown in Figures 2-4. As expected, the size of final product was found to be inversely proportional to the percent of Na₂PdCl₄ conversion.

These results indicate the successful size control of Pd nanoparticles relied on our capability in varying the percent conversion of Na₂PdCl₄ at the initial stage of a synthesis. Experimentally, based upon the conditions for synthesis of 5.3 nm Pd nanoparticles, our strategy to reduce the size for final products (*e.g.*, the 2.1 and 3.8 nm Pd nanoparticles shown in Figure 3) was to increase the amount of PVP (see Figure 1b). This is because PVP is a dual functional polymer that can serve as both colloidal stabilizer and reductant.^{57,58} When the amount of Na₂PdCl₄ is kept the same, the increase of PVP amount will enhance the reducing power of the reaction solution. As such, the percent conversion of Na₂PdCl₄ at the initial stage was increased, resulting in the reduction of particle size for final products.

On the other hand, our strategy to enlarge the particle size of final products (e.g., the 8.0, 10.9, 12.8, and 14.4 nm Pd nanoparticles shown in Figure 4) was to increase the amount of

Na₂PdCl₄ (see Figure 1c). It should be pointed out that, since the number and size of Pd nanoparticles were increased as more precursor was introduced, extra PVP was needed to stabilize the nanoparticles. Without extra PVP (*i.e.*, only increasing the amount of Na₂PdCl₄), nanoparticles were not effectively stabilized, leading to the formation of Pd nanoparticles with broad size distributions (see Figure S7). Similarly, only decreasing the amount of PVP without the change of Na₂PdCl₄ resulted in relative non-uniformity of the final products (Figure S8a). In the absence of PVP, the products became large aggregates and precipitates (Figure S8b). Therefore, the amounts Na₂PdCl₄ and PVP were spontaneously increased (see Table 1) for the synthesis of those larger Pd nanoparticles. In this case, despite the fact that more Pd(0) was generated at the initial stage due to the elevated concentrations of reactants, the excess amount of remaining Na₂PdCl₄ in the reaction solution ensured the decrease of the percent conversion of Na₂PdCl₄. As a result, the size of final products was enlarged.

Scale-up synthesis

Importantly, the synthesis could be readily scaled up to produce large quantities of Pd nanoparticles that are desired for industrial uses. Using the production of 5.3 nm (Figure 2) and 10.9 nm Pd nanoparticles (Figure 4b) as model examples, we scaled up the synthesis by 50 times, where a 500 mL flask was used as the reaction container (see Experimental Section for details). Figure 6 shows TEM images of the two products obtained from the scale-up synthesis, which were pretty uniform in both size and shape. The sizes of these products were measured to be almost the same as those obtained in small scale syntheses. Both products displayed a well-defined truncated octahedral shape. The quantities of Pd nanoparticles in Figure 6a and b were measured to be 0.28 and 2.81 gram, respectively, by ICP-MS analyses. These results suggest that the synthetic system could be easily scaled up, without the compromise of sample quality. In comparison, conventional seed-mediated growth could only produce Pd nanoparticles at the scale of several milligrams or less per batch.

Extension to other platinum-group metal nanoparticles

Finally, we also extended our synthetic strategy from Pd to other platinum-group metals, including Pt and Rh. The standard synthesis for Pt or Rh nanoparticles was performed using the same procedure for Pd nanoparticles shown in Figure 2, except for the substitution of Na₂PdCl₄ with the same molar amount of Na₂PtCl₄ or RhCl₃ as the precursor. As shown in Figure 7, Pt (Figure 7b) and Rh (Figure 7e) nanoparticles with good uniformities were obtained from the

standard synthesis. It should be mentioned that, unlike Pd case, as-synthesized Pt and Rh nanoparticles took overall spheroidal and multipod-like shapes, respectively, which were consistent with the results reported in previous work. 59,60 Significantly, just like the case of Pd, the sizes of these Pt and Rh nanoparticles could be conveniently tuned by adjusting the amount of PVP or precursor/PVP. For instance, when the amount of PVP in standard synthesis was increased by ten times while all other parameters were kept unchanged, the sizes of Pt and Rh nanoparticles were decreased (Figure 7a and d). The sizes of Pt and Rh nanoparticles could also be increased when the amounts of precursor and PVP in standard synthesis were spontaneously increased by ten times (Figure 7c and f). The low-magnification TEM images in Figure S9 demonstrate that all these Pt and Rh nanoparticles with different sizes could be obtained in high purities and large quantities. Collectively, these results suggest that our strategy of size control could be extended from Pd to Pt and Rh nanoparticles.

CONCLUSION

In conclusion, we have demonstrated a facile approach to the preparation of uniform Pd nanoparticles with controlled sizes in the range of 2-14 nm via one-pot synthesis. Ostwald ripening played a critical role in the growth process to ensure a narrow size distribution for the final products. The key to successful size control of Pd nanoparticles was to manipulate the percent conversion of Pd precursor at the initial stage of a synthesis. The synthesis could be readily scaled up to produce large quantities of Pd nanoparticles without the compromise of product quality. Notably, the strategy of size controlled synthesis could be extended to Pt and Rh nanoparticles. This work enables simple and large-scale production of uniform Pd nanoparticles with controllable sizes in common chemical laboratories, which will find immediate use in fundamental nanoresearch, catalysis, and biomedical research.

ASSOCIATED CONTENT

Supporting Information

Additional schematics and images. The Supporting Information is available free of charge on the ACS Publications website.

AUTHOR INFORMATION

Corresponding Author

*E-mail: Xiaohu.Xia@ucf.edu

Notes

The authors declare no competing financial interests.

ACKNOWLEDGEMENTS

This work was supported by a grant from the National Science Foundation (NSF, CBET 1804525), and the startup funds from the University of Central Florida. The XPS analysis work was partially supported by a NSF Major Research Instrumentation grant (ECCS 1726636). As a visiting graduate student from Beijing Jiaotong University, Y. Wang was partially supported by China Scholarship Council.

REFERENCES

- 1. Yin, L.; Liebscher, J. Carbon-Carbon Coupling Reactions Catalyzed by Heterogeneous Palladium Catalysts. *Chem. Rev.* **2007**, *107*, 133–173.
- 2. Chen, A.; Ostrom, C. Palladium-Based Nanomaterials: Synthesis and Electrochemical Applications. *Chem. Rev.* **2015**, *115*, 11999–12044.
- 3. Ge, C.; Fang, G.; Shen, X.; Chong, Y.; Wamer, W.; Gao, X.; Chai, Z.; Chen, C.; Yin, J. Facet Energy versus Enzyme-like Activities: The Unexpected Protection of Palladium Nanocrystals against Oxidative Damage. *ACS Nano* **2016**, *10*, 10436–10445.
- 4. Miller, M.; Askevold, B.; Mikula, H.; Kohler, R. H.; Pirovich, D.; Weissleder, R. Nanopalladium Is a Cellular Catalyst for *in vivo* Chemistry. *Nat. Commun.* **2017**, *8*, 15906.
- Chong, Y.; Dai, X.; Fang, G.; Wu, R.; Zhao, L.; Ma, X.; Tian, X.; Lee, S.; Zhang, C.; Chen,
 C.; Chai, Z.; Ge, C.; Zhou, R. Palladium Concave Nanocrystals with High-index Facets
 Accelerate Ascorbate Oxidation in Cancer Treatment. *Nat. Commun.* 2018, 9, 4861.

- 6. Dumas, A.; Couvreur, P. Palladium: A Future Key Player in the Nanomedical Field? *Chem Sci.* **2015**, *6*, 2153–2157.
- 7. Zhang, H.; Jin, M.; Xiong, Y.; Lim, B.; Xia, Y. Shape-Controlled Synthesis of Pd Nanocrystals and Their Catalytic Applications. *Acc. Chem. Res.* **2013**, *46*, 1783–1794.
- 8. Li, Y.; Boone, E.; El-Sayed, M. A. Size Effects of PVP–Pd Nanoparticles on the Catalytic Suzuki Reactions in Aqueous Solution. *Langmuir* **2002**, *18*, 4921–4925.
- 9. Lorenzo, M. P. Palladium Nanoparticles as Efficient Catalysts for Suzuki Cross-Coupling Reactions. *J. Phys. Chem. Lett.* **2012**, *3*, 167–174.
- Wilson, O. M.; Knecht, M. R.; Garcia-Martinez, J. C.; Crooks, R. M. Effect of Pd Nanoparticle Size on the Catalytic Hydrogenation of Allyl Alcohol. *J. Am. Chem. Soc.* 2006, 128, 4510–4511.
- 11. Semagina, N.; Renken, A.; Kiwi-Minsker, L. Palladium Nanoparticle Size Effect in 1-Hexyne Selective Hydrogenation. *J. Phys. Chem. C* **2007**, *111*, 13933–13937.
- 12. Jin, M.; Liu, H.; Zhang, H.; Xie, Z.; Liu, J.; Xia, Y. Synthesis of Pd Nanocrystals Enclosed by {100} Facets and with Sizes <10 nm for Application in CO Oxidation. *Nano Res.* **2011**, *4*, 83–91.
- Chen, B.; Crosby, L. A.; George, C.; Kennedy, R.; Schweitzer, N.; Wen, J.; Van Duyne, R. P.; Stair, P. C.; Poeppelmeier, K. R.; Marks, L. D.; Bedzyk, M. J. Morphology and CO Oxidation Activity of Pd Nanoparticles on SrTiO3 Nanopolyhedra. ACS Catal. 2018, 8, 4751–4760.
- 14. Zhou, W.; Lewera, A.; Larsen, R.; Masel, R. I.; Bagus, P. S.; Wieckowski, A. Size Effects in Electronic and Catalytic Properties of Unsupported Palladium Nanoparticles in Electrooxidation of Formic Acid. *J. Phys. Chem. B* **2006**, *110*, 13393–13398.
- 15. Zhou, W.; Lee, J. Y. Particle Size Effects in Pd-Catalyzed Electrooxidation of Formic Acid. *J. Phys. Chem. C* **2008**, *112*, 3789–3793.
- 16. Tang, S.; Chen, M.; Zheng, N. Sub-10-nm Pd Nanosheets with Renal Clearance for Efficient Near-Infrared Photothermal Cancer Therapy. *Small* **2014**, *10*, 3139–3144.
- 17. Zhou, C.; Long, M.; Qin, Y.; Sun, X.; Zheng, J. Luminescent Gold Nanoparticles with Efficient Renal Clearance. *Angew. Chem., Int. Ed.* **2011**, *50*, 3168–3172.
- 18. Adams, C. P.; Walker, K. A.; Obare, S. O.; Docherty, K. M. Size-dependent Antimicrobial Effects of Novel Palladium Nanoparticles. *PLoS One* **2014**, *9*, e85981.

- 19. An, K.; Somorjai, G. A. Size and Shape Control of Metal Nanoparticles for Reaction Selectivity in Catalysis. *ChemCatChem* **2012**, *4*, 1512–1524.
- 20. Teranishi, T.; Miyake, M. Size Control of Palladium Nanoparticles and Their Crystal Structures. *Chem. Mater.* **1998**, *10*, 594–600.
- 21. Ho, P.; Chi, K. Size-controlled Synthesis of Pd Nanoparticles from β-diketonato Complexes of Palladium. *Nanotechnology* **2004**, *15*, 1059–1064.
- 22. Sawoo, S.; Srimani, D.; Dutta, P.; Lahiri, R.; Sarkar, A. Size Controlled Synthesis of Pd Nanoparticles in Water and Their Catalytic Application in C–C Coupling Reactions. *Tetrahedron* **2009**, *65*, 4367–4374.
- 23. Roy, P.; Bagchi, J.; Bhattacharya, S. K. Size-controlled Synthesis and Characterization of Polyvinyl Alcohol Coated Palladium Nanoparticles. *Transit. Metal Chem.* **2009**, *34*, 447–453.
- 24. Qian, K.; Zhai, P.; Xian, J.; Hua, Q.; Chen, K.; Huang, W. Size Controlled Synthesis of Pd Nanoparticles Inspired from the Wacker Reaction and Their Catalytic Performances. *Catal. Commun.* **2011**, *15*, 56–59.
- 25. Wu, L.; Lian, H.; Willis, J. J.; Goodman, E. D.; McKay, I. S.; Qin, J.; Tassone, C. J.; Cargnello, M. Tuning Precursor Reactivity toward Nanometer-Size Control in Palladium Nanoparticles Studied by in Situ Small Angle X-ray Scattering. *Chem. Mater.* 2018, 30, 1127–1135.
- 26. Lu, L.; Wang, H.; Xi, S.; Zhang, H. Improved Size Control of Large Palladium Nanoparticles by a Seeding Growth Method. *J. Mater. Chem.* **2002**, *12*, 156–158.
- 27. Liu, J.; He, F.; Gunn, T. M.; Zhao, D.; Roberts, C. B. Precise Seed-Mediated Growth and Size-Controlled Synthesis of Palladium Nanoparticles Using a Green Chemistry Approach. *Langmuir* **2009**, *25*, 7116–7128.
- 28. Zhang, L.; Wang, L.; Jiang, Z.; Xie, Z. Synthesis of Size-controlled Monodisperse Pd Nanoparticles via A Non-aqueous Seed-mediated Growth. *Nanoscale Res. Lett.* **2012**, *7*, 312.
- 29. Xia, Y.; Gilroy, K. D.; Peng, H.; Xia, X. Seed-Mediated Growth of Colloidal Metal Nanocrystals. *Angew. Chem., Int. Ed.* **2017**, *56*, 60–95.
- 30. Xian, J.; Hua, Q.; Jiang, Z.; Ma, Y.; Huang, W. Size-Dependent Interaction of the Poly(*N*-vinyl-2-pyrrolidone) Capping Ligand with Pd Nanocrystals. *Langmuir* **2012**, *28*, 6736–6741.
- 31. Domínguez-Domínguez, S.; Berenguer-Murcia Á.; Pradhan, B. K.; Linares-Solano, Á.; Cazorla-Amorós, D. Semihydrogenation of Phenylacetylene Catalyzed by Palladium

- Nanoparticles Supported on Carbon Materials. J. Phys. Chem. C 2008, 112, 3827–3834.
- 32. Ślouf, M.; Pavlova, E.; Bhardwaj, M.; Pleštil J.; Onderková, H.; Philimonenko, A. A.; Hozák, P. Preparation of Stable Pd Nanoparticles with Tunable Size for Multiple Immunolabeling in Biomedicine. *Mater. Lett.* **2011**, *65*, 1197–1200.
- 33. Baeza, J. A.; Calvo, L.; Rodriguez, J. J.; Gilarranz, M. A. Catalysts Based on Large Size-Controlled Pd Nanoparticles for Aqueous-Phase Hydrodechlorination. *Chem. Eng. J.* **2016**, *294*, 40–48.
- 34. Hokenek, S.; Kuhn, J. N. Methanol Decomposition over Palladium Particles Supported on Silica: Role of Particle Size and Co-Feeding Carbon Dioxide on the Catalytic Properties. *ACS Catal.* **2012**, *2*, 1013–1019.
- 35. Wang, Y.; Peng, H.; Liu, J.; Huang, C.; Xia, Y. Use of Reduction Rate as a Quantitative Knob for Controlling the Twin Structure and Shape of Palladium Nanocrystals. *Nano Lett.* **2015**, *15*, 1445–1450.
- 36. Timoshkin, A. Y.; Kudrev, A. G. Calculations of Microconstants and Equilibrium Formation Constants for Platinum(II) and Palladium(II) Halide Complexes in Solution. *Russ. J. Inorg. Chem.* **2012**, *57*, 1362–1370.
- 37. Wulff, G. XXV. Zur Frage der Geschwindigkeit des Wachsthums und der Auflösung der Krystallflächen. Z. Kristallogr. 1901, 34, 449.
- 38. Marks, L. D. Experimental Studies of Small Particle Structures. *Rep. Prog. Phys.* **1994**, *57*, 603–649.
- 39. Xia, Y.; Xia, X.; Peng, H. Shape-Controlled Synthesis of Colloidal Metal Nanocrystals: Thermodynamic versus Kinetic Products. *J. Am. Chem. Soc.* **2015**, *137*, 7947–7966.
- 40. Sun, C.; Cao, Z.; Wang, J.; Lin, L.; Xie, X. Shape and Ligand Effect of Palladium Nanocrystals on Furan Hydrogenation. *New J. Chem.* **2019**, *43*, 2567–2574.
- 41. Xia, Y.; Xiong, Y.; Lim, B.; Skrabalak, S. E. Shape-Controlled Synthesis of Metal Nanocrystals: Simple Chemistry Meets Complex Physics? *Angew. Chem., Int. Ed.* **2008**, *48*, 60–103.
- 42. Gniewek A.; Trzeciak, A. M.; Ziółkowski, J. J.; Kępiński, L.; Wrzyszcz, J.; Tylus, W. Pd-PVP Colloid as Catalyst for Heck and Carbonylation Reactions: TEM and XPS Studies. *J. Catal.* **2005**, *229*, 332–343.
- 43. Ye, H.; Liu, Y.; Chhabra, A.; Lilla, E.; Xia, X. Polyvinylpyrrolidone (PVP)-Capped Pt

- Nanocubes with Superior Peroxidase-Like Activity. *ChemNanoMat* **2016**, *3*, 33–38.
- 44. Peng, H.; Xie, S.; Park, J.; Xia, X.; Xia, Y. Quantitative Analysis of the Coverage Density of Br⁻ Ions on Pd{100} Facets and Its Role in Controlling the Shape of Pd Nanocrystals. *J. Am. Chem. Soc.* **2013**, *135*, 3780–3783.
- 45. Xi, Z.; Ye, H.; Xia, X. Engineered Noble-Metal Nanostructures for *in Vitro* Diagnostics. *Chem. Mater.* **2018**, *30*, 8391–8414.
- 46. Niu, Z.; Li, Y. Removal and Utilization of Capping Agents in Nanocatalysis. *Chem. Mater.* **2014**, *26*, 72–83.
- 47. Crespo-Quesada, M.; Andanson, J. M.; Yarulin, A.; Lim, B.; Xia, Y.; Kiwi-Minsker, L. UV-Ozone Cleaning of Supported Poly(vinylpyrrolidone)-Stabilized Palladium Nanocubes: Effect of Stabilizer Removal on Morphology and Catalytic Behavior. *Langmuir* **2011**, *27*, 7909–7916.
- 48. Li, D.; Wang, C.; Tripkovic, D.; Sun, S.; Markovic, N. M.; Stamenkovic, V. R. Surfactant Removal for Colloidal Nanoparticles from Solution Synthesis: The Effect on Catalytic Performance. *ACS Catal.* **2012**, *2*, 1358–1362.
- 49. Naresh, N.; Wasim, F. G.; Ladewig, B. P.; Neergat, M. Removal of Surfactant and Capping Agent from Pd Nanocubes (Pd-NCs) Using Tert-butylamine: Its Effect on Electrochemical Characteristics. *J. Mater. Chem. A* **2013**, *1*, 8553–8559.
- 50. Naresh, N.; Wasim F. G. S.; Bradley, P. L.; Neergat, M. Sodium Borohydride Treatment: A Simple and Effective Process for the Removal of Stabilizer and Capping Agents from Shape-Controlled Palladium Nanoparticles. *Chem. Commun.* **2014**, *50*, 9365–9368.
- 51. Du, Y.; Yang, P.; Mou, Z.; Hua, N.; Jiang, L. Thermal Decomposition Behaviors of PVP Coated on Platinum Nanoparticles. *J. Appl. Ploym. Sci.* **2006**, *99*, 23–26.
- 52. Sun, Y.; Xia, Y. Triangular Nanoplates of Silver: Synthesis, Characterization, and Use as Sacrificial Templates For Generating Triangular Nanorings of Gold. *Adv. Mater.* **2003**, *15*, 695–699.
- 53. Gentry, S. T.; Kendra, S. F.; Bezpalko, M. W. Ostwald Ripening in Metallic Nanoparticles: Stochastic Kinetics. *J. Phys. Chem. C* **2011**, *115*, 12736–12741.
- 54. Frenken, J. W. M.; Stoltze, P. Are Vicinal Metal Surfaces Stable? *Phys. Rev. Lett.* **1999**, *82*, 3500.
- 55. Watzky, M. A.; Finke, R. G. Transition Metal Nanocluster Formation Kinetic and

- Mechanistic Studies. A New Mechanism When Hydrogen Is the Reductant: Slow, Continuous Nucleation and Fast Autocatalytic Surface Growth. *J. Am. Chem. Soc.* **1997**, *119*, 10382–10400.
- 56. LaMer, V. K.; Dinegar, R. H. Theory, Production and Mechanism of Formation of Monodispersed Hydrosols. *J. Am. Chem. Soc.* **1950**, *72*, 4847–4854.
- 57. Xiong, Y.; Washio, I.; Chen, J.; Cai, H.; Li, Z.; Xia, Y. Poly(vinyl pyrrolidone): A Dual Functional Reductant and Stabilizer for the Facile Synthesis of Noble Metal Nanoplates in Aqueous Solutions. *Langmuir* **2006**, *22*, 8563–8570.
- 58. Koczkur, K. M.; Mourdikoudis, S.; Polavarapu, L.; Skrabalak, S. E. Polyvinylpyrrolidone (PVP) in Nanoparticle Synthesis. *Dalton Trans.* **2015**, *44*, 17883–17905.
- 59. Herricks, T.; Chen, J.; Xia, Y. Polyol Synthesis of Platinum Nanoparticles: Control of Morphology with Sodium Nitrate. *Nano Lett.* **2004**, *4*, 2367–2371.
- 60. Zhang, H.; Xia, X.; Li, W.; Zeng, J.; Dai, Y.; Yang, D.; Xia, Y. Facile Synthesis of Five-fold Twinned, Starfish-like Rhodium Nanocrystals by Eliminating Oxidative Etching with a Chloride-Free Precursor. *Angew. Chem. Int. Ed.* **2010**, *49*, 5296–5300.

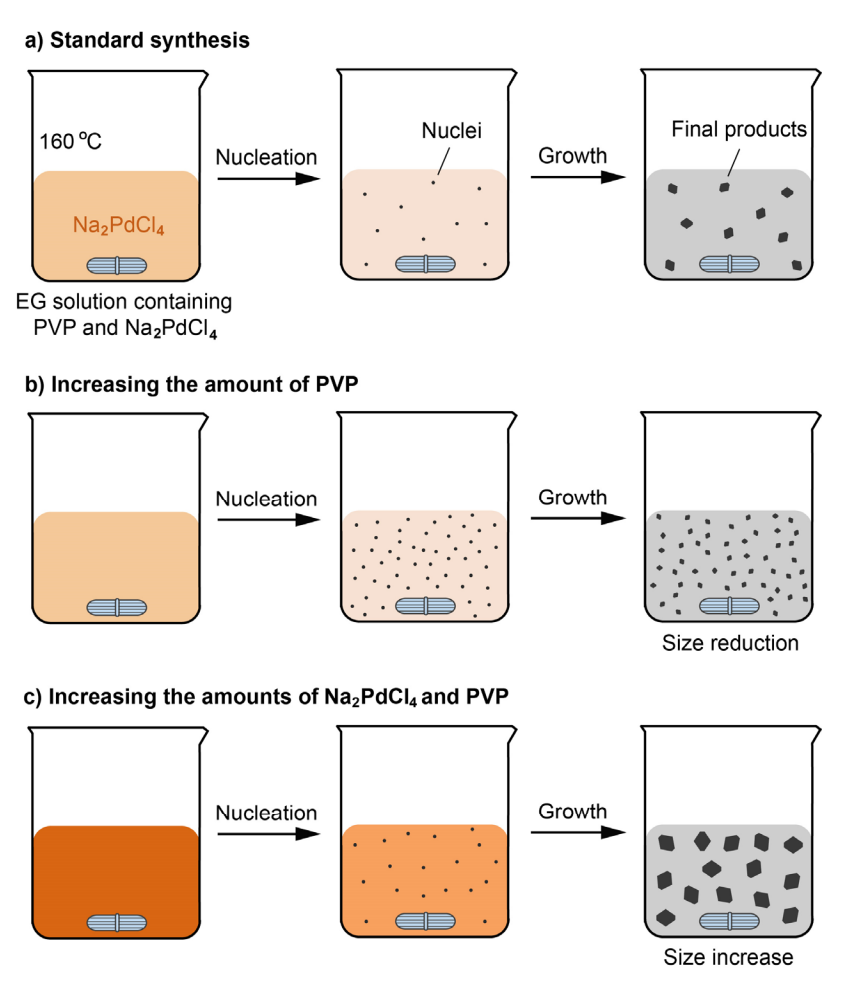


Figure 1. Schematics showing the synthesis of Pd nanoparticles with controlled sizes. (a) Standard synthesis for Pd nanoparticles; (b) Size reduction of Pd nanoparticles by increasing the amount of PVP in a standard synthesis; (c) Size increase of Pd nanoparticles by spontaneously increasing the amounts of Na₂PdCl₄ and PVP in a standard synthesis. In (a-c), brown color indicates Na₂PdCl₄ in EG solution, where the color intensity denotes the concentration of Na₂PdCl₄. The nuclei and nanoparticles as final products were not drawn to scale.

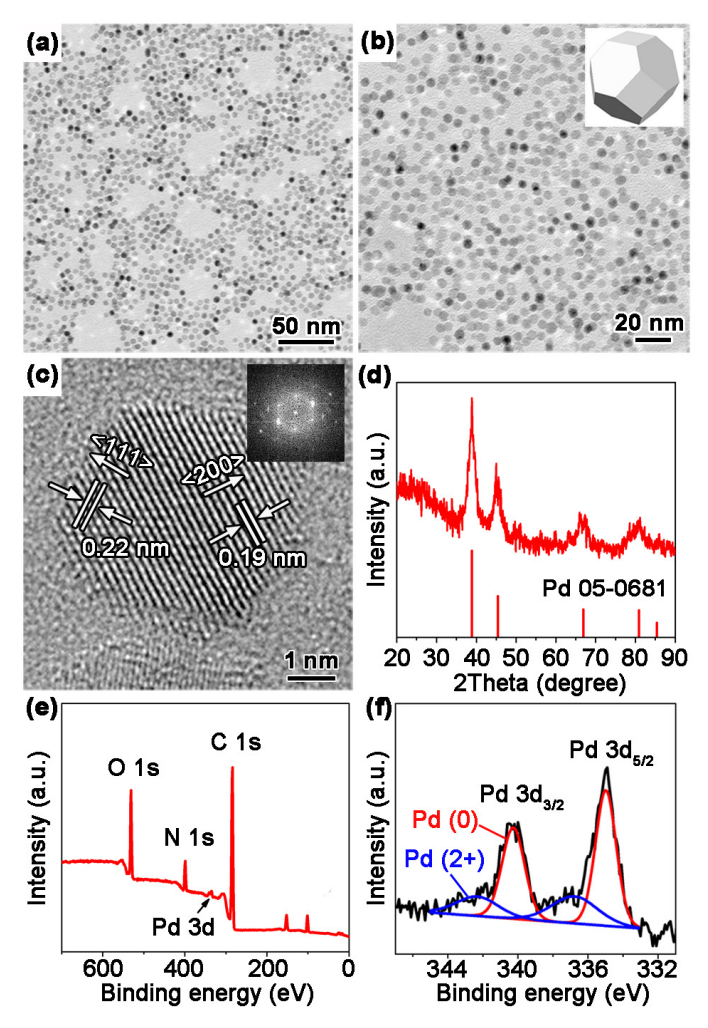


Figure 2. Pd nanoparticles with an average size of 5.3 nm that were prepared in a standard synthesis. (a) Low-magnification TEM image; (b) Magnified TEM image. Inset shows a 3D model of the sample; (c) HRTEM image of an individual Pd nanoparticle orientated along the <110> direction. The inset is the corresponding Fourier transform pattern; (d) XRD pattern. Red bars: JCPDS no. 05-0681 (Pd); (e) XPS survey spectra; (f) high resolution XPS spectra of the Pd 3d region.

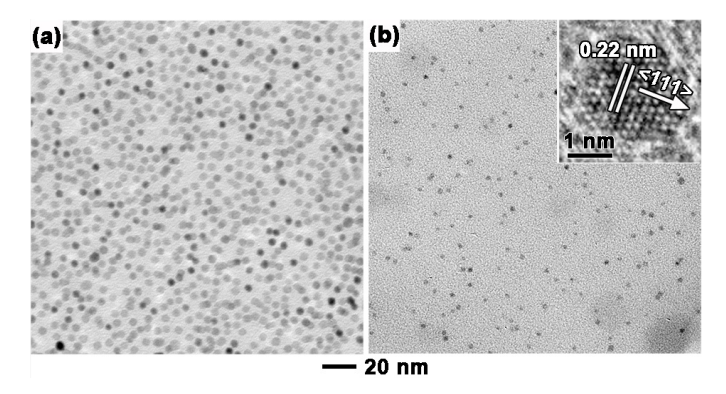


Figure 3. Pd nanoparticles with sizes smaller than 5.3 nm that were prepared by varying the amount of PVP in a standard synthesis as specified in Table 1. (a) 3.8 nm Pd nanoparticles; (b) 2.1 nm Pd nanoparticles. Inset in (b) is the HRTEM image of an individual Pd particle. The 20 nm scale bar applies to both images in (a) and (b).

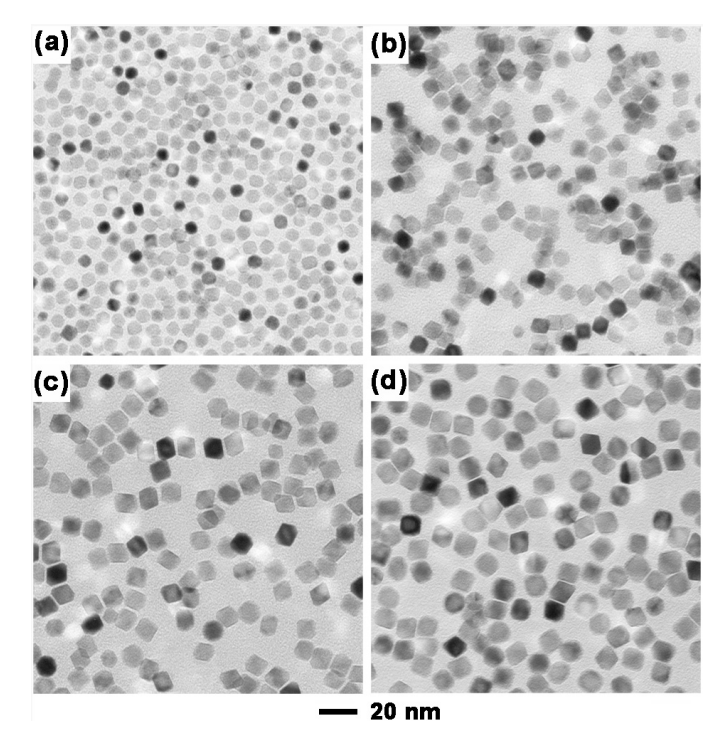


Figure 4. Pd nanoparticles with sizes larger than 5.3 nm that were prepared by increasing the amounts of Na₂PdCl₄ and PVP in a standard synthesis as specified in Table 1. (a) 8.0 nm Pd nanoparticles; (b) 10.9 nm Pd nanoparticles; (c) 12.8 nm Pd nanoparticles; (d) 14.4 nm Pd nanoparticles. The 20 nm scale bar applies to all images in (a-d).

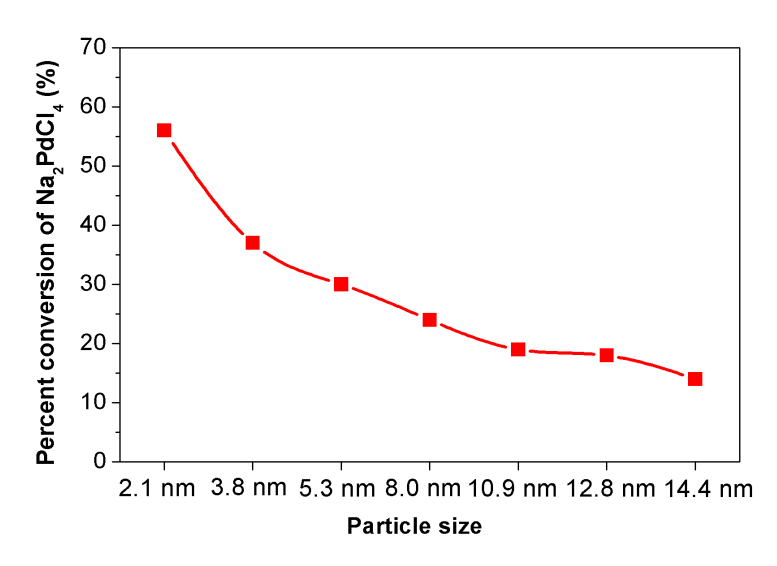


Figure 5. A plot showing the percent conversion of Na₂PdCl₄ to Pd(0) at the initial stage of synthesis as a function of the size of Pd nanoparticles obtained from the synthesis.

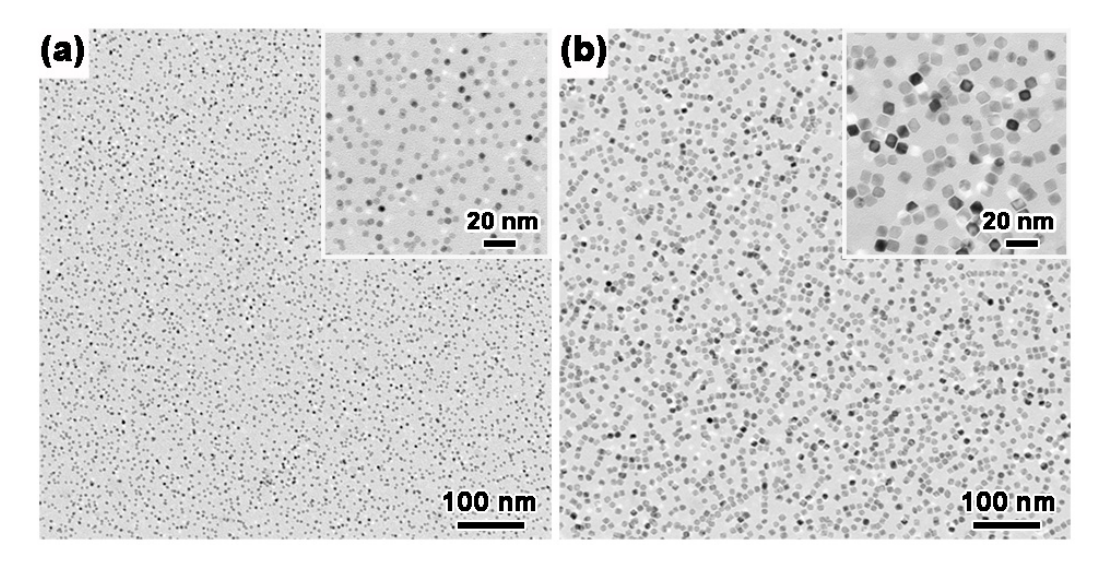


Figure 6. TEM images of Pd nanoparticles prepared from 50-fold scale up synthesis. (a) 5.3 nm Pd nanoparticles; (b) 10.9 nm Pd nanoparticles. Insets in (a) and (b) are TEM images of the same samples at higher magnifications.

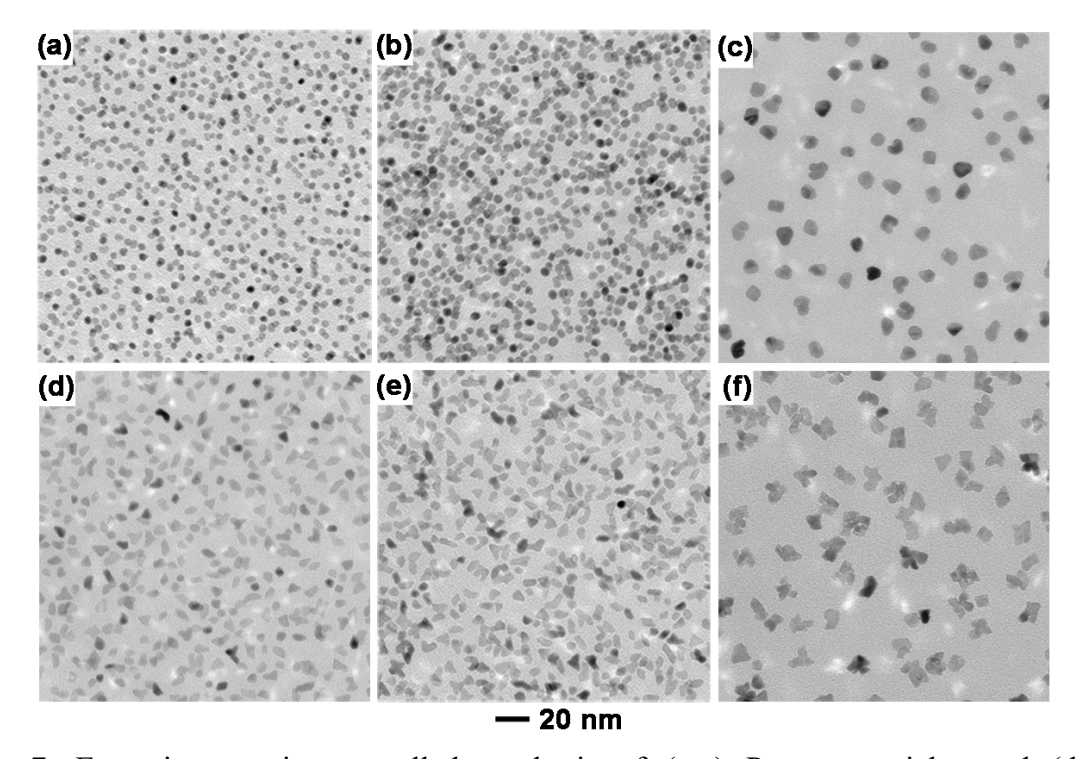


Figure 7. Extension to size-controlled synthesis of (a-c) Pt nanoparticles and (d-f) Rh nanoparticles. Samples in (b) and (e) were synthesized using the procedure for preparing 5.3 nm Pd nanoparticles shown in Figure 2, except for the substitution of Na₂PdCl₄ with the same molar amounts of Na₂PtCl₄ (b) and RhCl₃ (e) as precursors; Samples in (a) and (d) were synthesized using the same procedures for samples in (b) and (e), respectively, except that the amount of PVP was increased by ten times; Samples in (c) and (f) were synthesized using the same procedures for samples in (b) and (e), respectively, except that the amounts of precursors and PVP were spontaneously increased by ten times. The 20 nm scale bar applies to all images in (a-f).

Table 1. Synthetic conditions for the Pd nanoparticles of different sizes displayed in Figures 2-4. The standard synthesis for 5.3 nm Pd nanoparticles is highlighted in gray.

Size of Pd nanoparticles (nm)	Amount of PVP in 2.0 mL EG (mg)	Amount of Na ₂ PdCl ₄ in 1.0 mL EG (mg)	Molar ratio of PVP to Pd	Temperatu re (°C)	Reaction time (h)
2.1	1,600	16	0.53	160	1.0
3.8	200	16	0.067	160	1.0
5.3	40	16	0.013	160	1.0
8.0	200	80	0.013	160	1.0
10.9	400	160	0.013	160	1.0
12.8	800	324	0.013	160	1.0
14.4	1,200	480	0.013	160	1.0